

Marco Atzori · Andrea Nistri

Non-monotonic decay of excitatory synaptic transmission in the frog optic tectum following repetitive stimulation of the optic nerve in vitro

Received: 21 February 1994 / Accepted: 28 August 1994

Abstract The monosynaptic field excitatory postsynaptic potentials (EPSPs) evoked in the optic tectum of the frog (*Rana temporaria*) in vitro by different patterns of stimulation of the contralateral optic nerve were studied using extracellular recording. Pulse trains at frequencies of less than or equal to 0.033 Hz elicited field potentials of stable amplitude, whereas in the range 0.33–1.0 Hz EPSPs showed a depression in the first few responses subsequent to the first one, followed by a partial recovery and a final decline to a steady level. When the inter-pulse interval was less than 200 ms, paired-pulse monosynaptic facilitation was found. Decrease in the external Ca^{2+} concentration, or in the stimulation intensity or application of picrotoxin reversibly produced a monotonically decreasing EPSP amplitude, suggesting that a local neuronal circuit was controlling the development of synaptic fatigue. A simple model based on the combined effects of depletion of excitatory transmitter stores plus activation of a local inhibitory circuit was found to provide a simulation which closely resembled the experimentally observed pattern of synaptic fatigue. The present study suggests that an inhibitory synaptic process contributed to the non-monotonic decay of excitatory transmission in the frog optic tectum, following repetitive stimulation of the optic nerve.

Key words Fatigue · Local circuitry · Inhibition GABA · Frog

Introduction

Short-term changes in synaptic transmission following repetitive stimulation have been extensively studied at the vertebrate neuromuscular junction, in which the

purely monosynaptic innervation by a motor axon to muscle fibres simplifies these investigations. Facilitation, depression, potentiation and related phenomena can therefore be separately observed, taking into account the possible overlapping of their time course (for a review see, for instance, Magleby 1987). Similar processes in the central nervous system are comparatively less well understood, because of a variety of factors. For instance, in visual areas of mammals, habituation of cortical neurones to sensory inputs is partially due to a decreased efficiency in synaptic transmission (intrinsic synaptic fatigue) as well as to the influence of a local network (Maddess et al. 1988; Vidysagar 1990). Likewise, in the frog brain, adaptation of primary visual neurones of the optic tectum (OT) to retinal inputs develops quickly, although the underlying mechanism remains unclear (Maturana et al. 1960). The present investigation focused on the process of synaptic fatigue in the frog OT, since the visual system of this animal presents some rather interesting characteristics. In particular, it contains different types of retinal ganglion cells supplying brain neurones with visual signals segregated into four main classes of optic nerve axons (Maturana et al. 1960). When a recording microelectrode is advanced through the amphibian OT, it will pick up discrete responses comprising the signal from distinct optic nerve afferents and from the excitatory synapses established by these fibres in separate layers of the OT. Such an anatomical arrangement will ensure that pure monosynaptic excitatory responses can be selectively recorded from different layers of the OT. This situation was amply investigated by Chung et al. (1974), who observed four monosynaptic excitatory potentials uncontaminated by local network signals when single pulses of varying strength and duration were delivered to the optic nerve. Chung et al. (1974) also provided a systematic classification of these monosynaptic potentials on the basis of their origin due to activation of either fast (myelinated) or slow (unmyelinated) fibres. According to this study monosynaptic potentials are conventionally referred to as m_1 and m_2 or u_1 and u_2 , depending on the myelinated

M. Atzori · A. Nistri (✉)
Biophysics Laboratory,
International School for Advanced Studies (S.I.S.S.A.),
via Beirut 2/4, I-34014 Trieste, Italy;
FAX no: 39–40–3787–528

or unmyelinated nature of their presynaptic fibres (subscript 1 or 2 indicates the latency from the stimulus artefact). In addition to the primary relay neurones the OT also contains many other cell types. For instance, immunohistochemical studies show a highly developed GABAergic system (Antal 1991), which may provide an inhibitory control, particularly when repetitive activity is elicited by relatively high frequency impulses of the optic nerve. The frog OT is therefore a preparation suitable for investigations into the effects of a local inhibitory network on fatigue of excitatory transmission, which is thought to be mediated mainly by glutamate (Nistri et al. 1990). Experimental advantages in using a frog OT preparation include: (a) the anatomically homogeneous sensory input by the optic nerve (without efferent fibers) establishing monosynaptic contacts with tectal neurones (Chung 1974); (b) the nearly complete crossover of the optic nerve tectal afferents at the chiasma and the distinct laminar organization of the OT with layer-specific distribution of the optic nerve afferents (Lázár 1984); (c) long survival *in vitro* with fully maintained synaptic transmission. Of course, like any preparation of central nervous system in which its architecture is left intact in order to study synaptic transmission, experimental problems arise from the multisynaptic arrangement of sensory inputs which can hardly be regarded similar to the simple situation found, for instance, at the frog neuromuscular junction. Nevertheless, if relatively simple, basic properties of synaptic transmission at peripheral junctions can be applied to central synapses, even integrated responses such as those displayed by visual neurones may be interpreted in the light of these findings. For this purpose, the present study sought: (1) to examine some general properties of synaptic fatigue produced by repeated stimulation of the optic nerve, (2) to compare them with other forms of short-term changes in synaptic transmission and (3) to attempt the construction of a model reproducing the experimental observations on the basis of the possible involvement of a local inhibitory network.

Materials and methods

Thirty-one adult frogs (*Rana temporaria*) were anaesthetized in a 0.1% tricaine solution and decapitated. The brain was removed, the telencephalon destroyed and the remaining mid-brain preparation was superfused in a recording chamber with frog Ringer solution containing NaCl 111 mM, KCl 2.5 mM, NaHCO₃ 17 mM, NaH₂PO₄ 0.1 mM, CaCl₂ 2.5 mM and glucose 4 mM. 'Low Ca²⁺' solution consisted of 1.75 mM CaCl₂ plus 0.75 mM MgCl₂. Picrotoxin (75 µM) was used to block chloride-mediated inhibitory processes (Sivilotti and Nistri 1991). The solution was oxygenated with a mixture of 95% O₂ and 5% CO₂ (pH 7.3); the bath temperature was kept between 9 and 10°C. One millisecond-long stimuli were applied to the contralateral optic nerve through a low-resistance suction electrode. The recording electrode, filled with 3 M NaCl, had a resistance of 2–10 MΩ and was placed at a depth of 100 µm from the outer surface of the OT. Evoked excitatory postsynaptic potentials (EPSPs; 0.3–3.0 mV) were amplified with an Axoclamp 2A unit and further 200-fold amplified before being digitized at 4 kHz by a Labmaster interface connected to an

IBM-PC computer. Both acquisition and signal analysis were performed using pCLAMP software (version 5.5) in the pulse mode. Optic nerve stimulation elicited a signal consisting of one or more of three waveforms at different latencies, named m_2 , u_1 and u_2 (Chung et al. 1974). Because of their possible overlap, the amplitude of the peak m_2 and u_1 responses and the response of the u_2 at about 150 ms from the stimulus artefact were measured (with respect to the baseline taken as the voltage level 50 ms before the stimulus artefact) rather than their integrals. In fact, the integral method would be much less reliable, as each one of the overlapping waves would have to be subtracted from the others after the estimation of its isolated shape. It was therefore more accurate to measure the peak value of the waves because of negligible overlap in the peak regions. The data are given as means \pm SEM. Statistical analysis of related samples was done using Student's *t*-test for the differences for numerical values and the Wilcoxon test for the differences in ranked measures (Colquhoun 1971). Only differences with $P < 0.05$ were accepted as significant. Experimental data were fitted with a linear least-squares routine implemented with a Pascal program. The goodness of fit was evaluated with the Chi-square test. All calculations were performed with an IBM-PC.

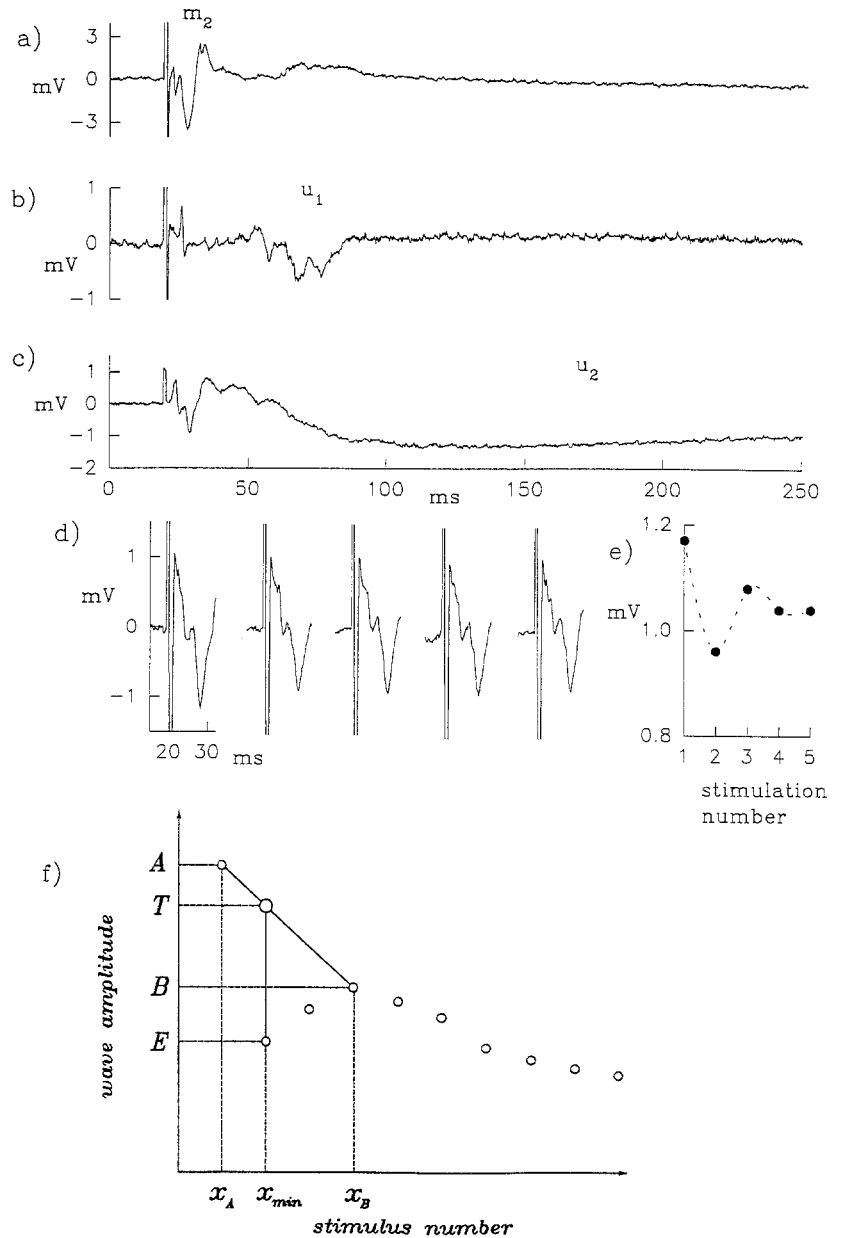
Results

General characteristics of responses evoked by the optic nerve

Following stimulation of the contralateral optic nerve, m_2 , u_1 and u_2 waves were detected with latencies of 9.9 ± 1.0 ms, 41.9 ± 2.5 ms and more than 120 ms, respectively (Fig. 1a–c); whereas the m_1 wave was not observed. The identification of these field potentials as the pure monosynaptic excitatory responses previously described was based on their current density analysis and their level of polarity reversal, which was the same as reported by Chung et al. (1974). While all preparations displayed reliably recorded m_2 and u_1 waves, the u_2 wave was detected less frequently under the present experimental conditions of recording depth and stimulus strength (Chung et al. 1974).

The reproducibility of measurements was tested at the beginning of each experiment by stimulating at very low frequencies (0.033 Hz), which consistently induced stable waveforms. A minimum of 60 s was consequently chosen as a safe interval to obtain recovery from any modifications produced by higher frequency pulses. Under these circumstances the amplitude of the synaptic waveforms showed minimal variability and, in particular, no appreciable change in the time to peak. These observations indicate that the stimulation parameters were adequate to provide reliable, stable activation of the optic nerve fibres. Input/output curves were constructed by measuring the response amplitude to small increments in the stimulation intensity and were used for determining the stimulation threshold and the minimum stimulation intensity to induce a maximal response for each wave. Maximal stimulations were usually in the 10 to 40 V range, that is, at least 10 times larger than the threshold value for stimulation, although intensities up to 65 V were occasionally applied. Submaximal stimulations were defined as those eliciting 50–

Fig. 1a-f Synaptic field potentials recorded from the frog optic tectum in control saline solution. **a,b,c** Representative recordings of the m_2 , u_1 and u_2 , respectively, from three different preparations stimulated at 0.033 Hz. **d** Consecutive recordings of m_2 wave demonstrating its decay pattern following 1 Hz stimulation. **e** Plot of the changes in m_2 amplitude versus number of pulses in 1 Hz train for the experiment shown in **d**. Data-points were fitted with a spline curve. **f** Schematic diagram to show method to calculate variation from linear decay (VLD) during the early part of synaptic fatigue (see text); the *small circles* represent the experimentally observed points, the *large circle* is the interpolated response. A is the amplitude of first response, B is the largest amplitude of exponentially decaying responses, E is the smallest response before exponential decay. x_A , x_B and x_{min} are the corresponding stimulus numbers: T is the linear interpolation (at x_{min}) between values of A and B .



70% of the maximal response. Preparations showing reliable responses for at least 3 h were used, although the average survival of the preparations was much longer.

Trains of pulses at low frequency

Trains of 5–20 pulses at various frequencies (0.1–1.0 Hz) were applied to evoke responses which were averaged from four identical stimulation trains. While in 8 preparations a monotonic decay of synaptic transmission following train stimulation appeared, for the majority of preparations (23/31) the amplitude of the synaptic responses declined during the stimulus train in a non-monotonic fashion, since the initial few responses after the first one were essentially smaller than later ones be-

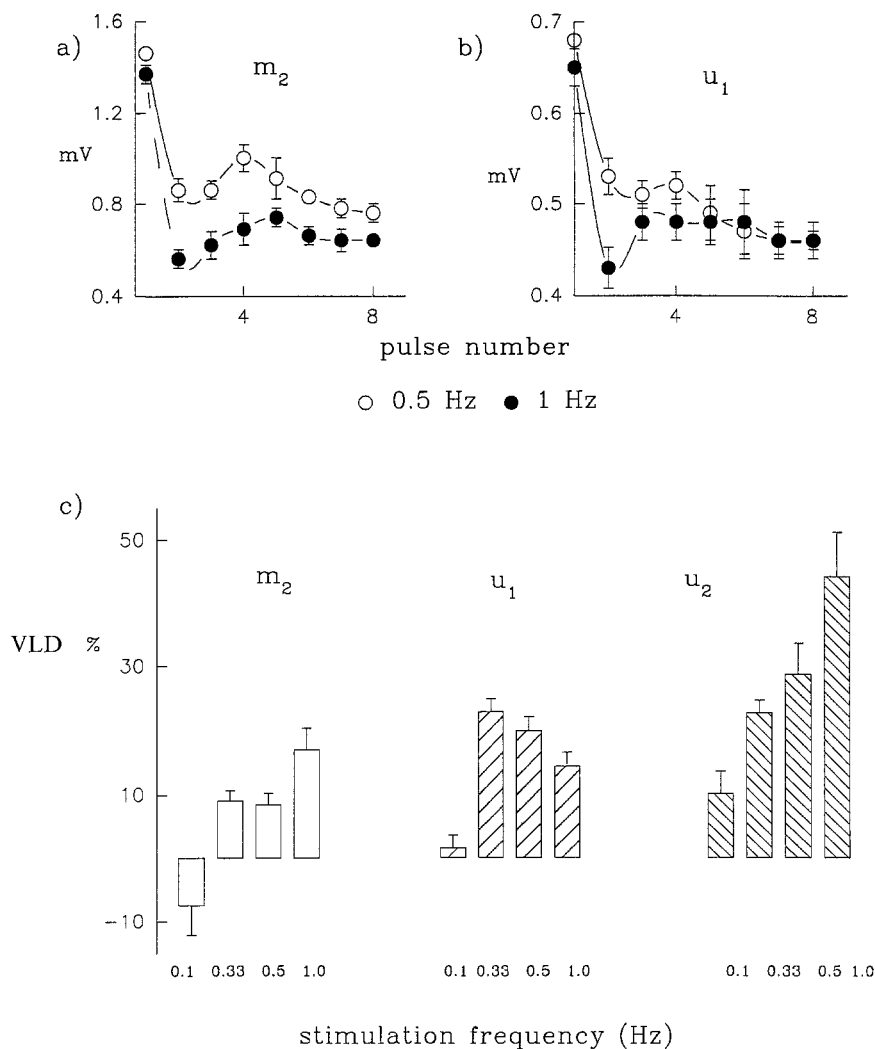
fore a steady state amplitude was eventually reached, giving the biphasic appearance shown in Fig. 2a,b.

The amplitude of this phenomenon was often directly related to the stimulation frequency, as shown in Fig. 2a. For a quantitative estimate of the non-monotonic decay of synaptic transmission, a simple parameter was calculated, namely the variation from the linear decay (VLD). VLD was defined as the difference between the interpolated value of the smallest response (assuming linear decay from the first one to the next largest response) and the observed amplitude of the same response (normalized to the first response); this is exemplified in Fig. 1f, where:

$$\text{VLD} = \frac{T - E}{A} \times 100$$

$$\text{with } T = m(x_{min} - x_A) + A \text{ and } m = \frac{B - A}{x_B - x_A}. \quad (1)$$

Fig. 2a–c Development of synaptic fatigue at different stimulation frequencies in control saline solution. **a,b** Pattern of synaptic fatigue at different frequencies (0.5 or 1.0 Hz) for the m_2 and the u_1 waves, respectively ($n=4$). Datapoints were fitted using a spline curve. **c** Histograms of changes in variation from linear decay for various stimulus frequencies shown at the bottom of each bar, generating the m_2 (left), u_1 (middle) and u_2 (right) synaptic waveforms ($n=7$).



At 0.1 Hz the VLD values for all three waves were rather small ($\leq 10\%$) or even negative in the case of the m_2 waveform (Fig. 2c). Raising the stimulation frequency to 1 Hz gave significant VLD increases for the three responses, whereas intermediate frequencies (0.33 Hz or 0.5 Hz) produced significant VLD values only for the u_1 response (Fig. 2c). Since at 1 Hz stimulation rate all the waves displayed the non-monotonic decay pattern (with full recovery after 60 s rest), experiments were carried out at this frequency to explore whether a local network might have been involved in synaptic fatigue. A polysynaptic system may be expected to require a certain stimulation threshold for its activation: the intensity of the stimuli was therefore reduced, with consequent decrement in postsynaptic response amplitude. Figure 3a,b demonstrates that weaker stimuli also elicited less fatigue and smaller variations in the early part of the decay pattern (Table 1), while the amplitude of the afferent volley elicited by strong pulses was found essentially unchanged for frequencies up to 1 Hz (Fig. 3a,b).

The dependence of synaptic fatigue on stimulation frequency was in keeping with the possibility that a local circuit played a role in this phenomenon. In this case

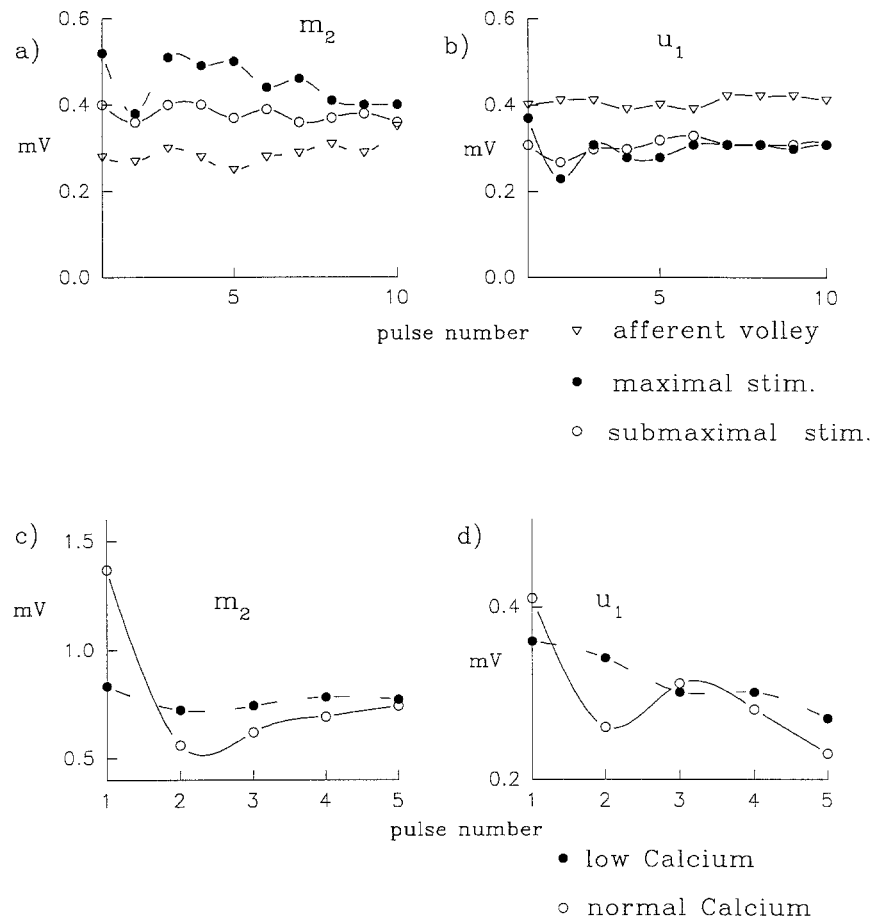
the activation of an interneuronal pathway would be expected to add responses which are more critically dependent on $[Ca^{2+}]_o$ than monosynaptic transmission. A reduction in $[Ca^{2+}]_o$ from 2.5 to 1.75 mM should therefore induce not only a decrease in the EPSP amplitude but also a much larger fall in the influence of any polysynaptic pathway. This phenomenon was in fact observed, as shown in Fig. 3c,d (Table 1).

A polysynaptic inhibitory pathway would possibly utilize GABA, a major neurotransmitter in the frog brain (Sivilotti and Nistri 1991), for this purpose. In order to block GABA receptor systems completely, picrotoxin (75 μ M) was added to the Ringer solution. In separate experiments this picrotoxin concentration was found to be the largest one just subthreshold for induction of convulsive activity. When tests for synaptic fatigue were performed, it was shown (Fig. 4) that after 10–15 min exposure to picrotoxin this phenomenon for the m_2 and the u_1 waves was less dramatic than in controls (Table 1) and lacked transient recovery. These results are thus comparable with those obtained in low- $[Ca^{2+}]_o$ solution or with submaximal stimulations.

Table 1 Change in values of variation from linear decay (VLD) during test treatments. Results are expressed as the difference between VLD data in control solution and those during one of the treatments listed in the first column. Values are arithmetic and geometric mean \pm SEM. *P* values were obtained with the Wilcoxon test on related samples (Colquhoun 1971). Data for the u_2 wave in picrotoxin solution are not included, as they were recorded from only two preparations

	Arithmetic mean	Geometric mean	<i>P</i> <	Number of experiments
Test for m_2				
Low Ca^{2+}	13.4 ± 3.5	12.0 ± 3.8	0.05	7
Submaximal stimulus	12.3 ± 3.8	11.1 ± 4.1	0.05	7
picrotoxin	13.0 ± 1.4	12.7 ± 1.7	0.05	7
Test for u_1				
Low Ca^{2+}	13.4 ± 4.2	12.5 ± 4.7	0.05	6
submaximal stimulation	20.1 ± 6.0	17.2 ± 6.4	0.05	6
picrotoxin	24.9 ± 2.3	23.7 ± 3.4	0.05	6
Test for u_2				
Low Ca^{2+}	31.6 ± 9.5	28.1 ± 10.7	0.05	6
submaximal stimulus	18.1 ± 4.1	14.8 ± 4.6	0.05	6

Fig. 3a–d Representative examples of differential sensitivity of the synaptic fatigue process to changes in stimulation intensity or $[\text{Ca}^{2+}]_o$. **a,b** Plot of changes in amplitude of the m_2 and u_1 waves versus pulse number in a train following strong or weak stimuli always applied at 1 Hz. The amplitude of the afferent volley (∇) recorded during the same experiment is also shown. Note that changes in amplitude are absent for the afferent volley, slight for the field potentials elicited by weak stimuli and much larger for the field potentials evoked by strong stimuli. All the data were fitted by a spline curve. **c,d** Reduction and smoothing of the synaptic fatigue process produced by strong stimuli at 1 Hz in a low- $[\text{Ca}^{2+}]_o$ solution (\bullet) for the m_2 (left) and u_1 (right) waves when compared with similar data recorded from the same preparation in control saline (\circ)



Paired-pulse facilitation

In the frog OT in vivo paired-pulse stimulation of the optic nerve at intervals of less than 1 s induces facilitation for all three synaptic waves (Chung et al. 1974). It was therefore necessary to check whether in vitro experiments demonstrated the same phenomenon and whether facilitation could partly influence the time course of synaptic fatigue. In the present experiments

the amount of facilitation was quite large, as shown in Fig. 5a. In order to avoid the problems caused by the overlapping of the different waves elicited by the pair of pulses, a control trace with only the first response was first digitized, and then a second trace with the two consecutive responses was obtained for each interpulse interval. Subtracting the first trace from the second one gave the amplitude of the facilitated response, which was normalized by dividing it by the first control re-

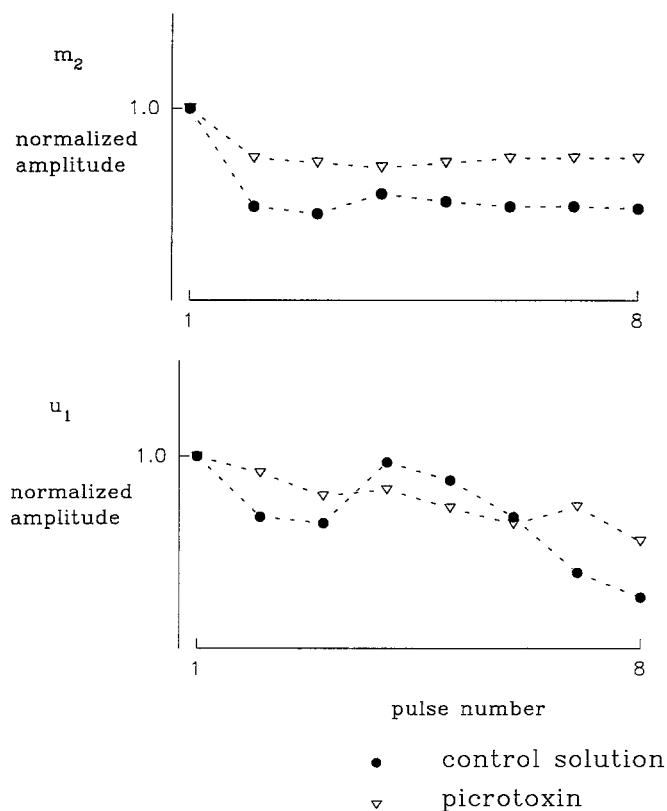


Fig. 4 Effect of 75 μ M picrotoxin on synaptic fatigue pattern. A representative experiment showing the time course of m_2 and u_1 waveforms (produced by strong stimuli at 1 Hz). Picrotoxin was added to control saline after recording drug-free responses (\bullet). Datapoints (joined by straight lines) in picrotoxin solution (∇) were obtained after 20–30 min exposure to this agent

sponse. Graphs showing facilitation as a function of the interpulse interval are reported in Fig. 5b–d. Both maximal and submaximal responses were found to be facilitated for pulses closer than 200 ms, but a different behaviour occurred at interpulse delays longer than 300–500 ms (Fig. 5e), since submaximal responses showed neither facilitation nor depression, while maximal responses replaced their facilitation with depression.

In order to provide a mathematical fit for the experimental data, we tested whether the model described for the frog neuromuscular junction could be applied to the frog OT. This approach seemed permissible in view of the spatial segregation of various synapses responsible for generating the different tectal field potentials. In line with this assumption facilitation (F) was defined as (Magleby 1987):

$$F = A_2/A_1 - 1 \quad (2)$$

where A_1 and A_2 are the amplitudes of the same wave elicited by the first and second pulse, respectively. To evaluate its time course, the following expression (Magleby 1987) was used:

$$\frac{dF}{dt} = J_0 f - r f \quad (3)$$

Table 2 Paired-pulse facilitation values. $T_{\max \text{ exper}}$ the intervals giving the maximal facilitation observed experimentally, $\%_{\max \text{ exper}}$ the experimental maximum facilitation of each waveform expressed as percentage of the first control response, f , τ meaning given in the text, Eq. 4

	m_2	u_1	u_2
$T_{\max \text{ exper}}$ (ms)	38 ± 15	74 ± 41	50
$\%_{\max \text{ exper}}$	120 ± 59	52 ± 18	59
f (%)	304 ± 165	59 ± 26	492
τ (ms)	49 ± 19	131 ± 61	35

in which J_i is the delta function corresponding to the pulses, f is the amount of facilitation per pulse and $r = 1/\tau$ is the rate constant for the removal of F . Other processes such as augmentation, potentiation or depression have not been included. Solution of eq. 3 for paired pulses is

$$F = f e^{-t/\tau} \quad (4)$$

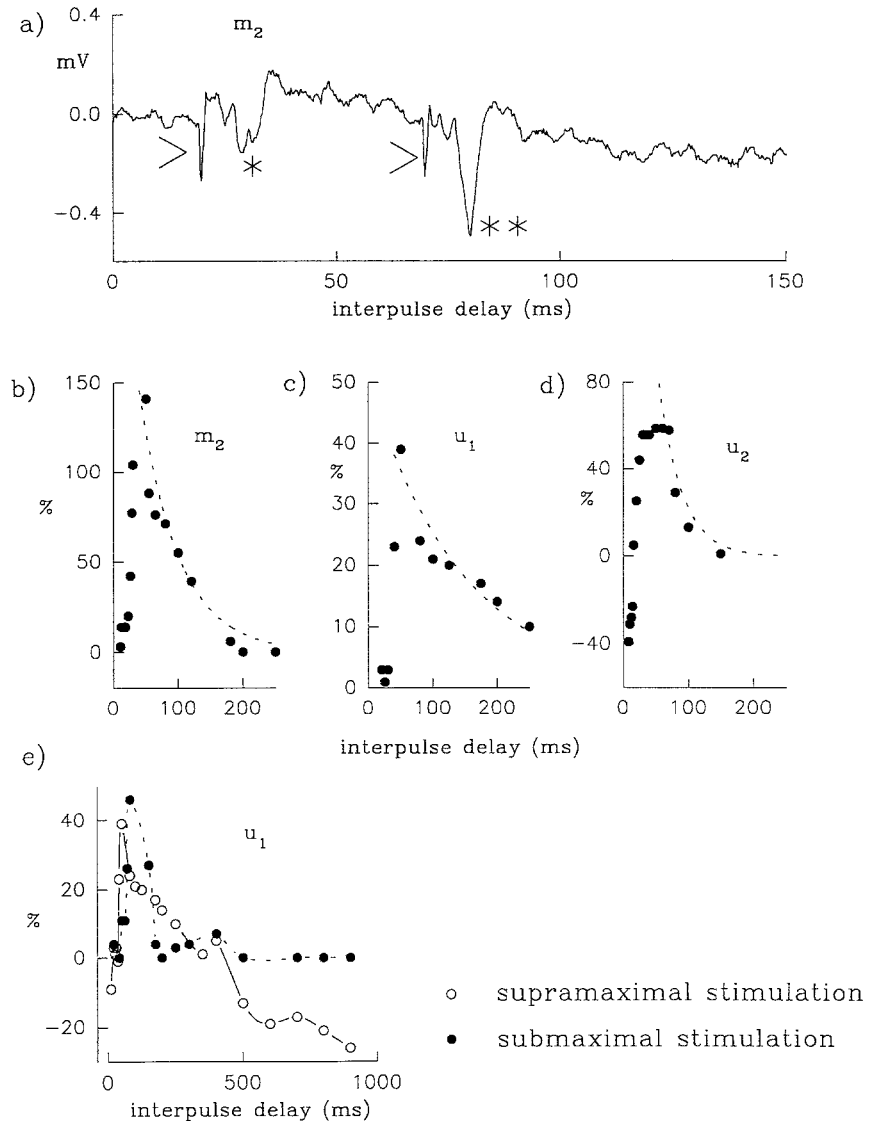
where t is the interval between pulses.

Facilitation peaked at less than 100 ms and was very small after 500 ms. Table 2 provides numerical values obtained for the fit. Although the limited accuracy of the field potential analysis does not allow to distinguish various components of the signal enhancement process, the present results confirm that it was essentially correct to use a stimulation frequency of up to 1 Hz for studying synaptic fatigue apparently uncontaminated by facilitation. The closeness of fit derived from Magleby's model with the experimental observations of paired-pulse facilitation suggested that the adopted minimal model adequately described the process without the requirement of introducing any more complex treatment.

A model for inhibition

In order to provide a simple description of synaptic fatigue observed following 1 Hz stimulation, various models were tested for their ability to simulate the experimental observations. To start with, we checked whether the simple process of depletion of a presynaptic immediately available store (IAS) of neurotransmitter (Llinàs et al. 1981) refilled from a long-term store (LTS) of infinite capacity (following first-order kinetics) could adequately describe synaptic fatigue of the OT. In this case the value of the rate constant (τ_{NT}) representing the kinetics of transfer between the two stores was set between 4 and 10 s. The simulated synaptic response declined with a single exponential pattern, which, although similar to the late time course of the fatigue, was unable to reproduce the initial non-monotonic decay. It was therefore necessary to devise more complex models. One of them considered that the refilling of the depleted store began with a variable delay ranging from values of less than or equal to interpulse frequency to twice τ_{NT} . With a suitable choice of refilling delay (4–8 s) and of

Fig. 5a–e Paired-pulse facilitation of excitatory transmission in the frog optic tectum. **a** Example of facilitation of the m_2 wave; compare response produced by 50 ms interpulse delay (**) with the one (*) obtained without prepulse; *arrows* show the stimulus artefact. **b–d** Facilitation of m_2 , u_1 and u_2 , respectively. Quantitative data for this phenomenon are reported in Table 2. *Dashed lines* represent the best-fit exponential for facilitation (see Eq. 4), while *filled circles* indicate experimental data. Intervals between pulses were chosen to be approximately 5–10 ms up to 100 ms intervals and 20–100 ms for larger intervals (up to 900 ms). Experimental points at smaller intervals than the one producing maximal facilitation were not used for the fit. **e** Spline curve plot of percentage facilitation of u_1 wave by strong (○) or weak (●) pulses versus interpulse delay. Note that after 500 ms synaptic depression occurred with strong pulses. All data were recorded in control saline



τ_{NT} (4 or 8 s), a biphasic response with an initial decay and a subsequent rise to a steady state level was generated, without the characteristic dip interrupting the empirically produced synaptic fatigue. A variation of this model was then introduced in the attempt to mimic the experimental observations: in such a case an intermediate neurotransmitter store was postulated to operate between IAS and LTS, with first-order kinetics governing the transfer between the three stores. This model improved the fit of the experimental data but completely failed to reproduce important experimental observations, for instance that the VLD values were strongly related to the stimulus strength. These results prompted the need to add to each response a decremting factor proportional to the amplitude of the preceding one. In practice this amounted to combining the first model (neurotransmitter released from IAS and refilled from LTS) with an inhibitory component generated by the preceding response and proportional to it.

Using these assumptions a set of equations (Eqs. A1–

A3; see Appendix) was employed to fit the time course of synaptic signals elicited during a train of stimuli. Figure 6 shows results of this type of fit and provides some parameters relevant for the description of the theoretical model. As indicated in Table 3, these were: τ_{NT} , i.e. the time constant for refilling of IAS by LTS; α , i.e. a dimensionless constant proportional to the amount of inhibition elicited by each stimulus; and τ_{inh} , i.e. the time constant of the decay of the inhibitory process evoked by each stimulus. Table 3A gives the mean \pm SEM of three fits obtained from four averaged responses of three preparations. A Chi-square test with $n-5$ degrees of freedom (n is the total number of points and 5 is the number of the fitting parameters plus the normalization condition) gave values acceptable within at least a 5% confidence level. For the least-squares minimization procedure the two trains of responses at maximal and submaximal stimulation were simultaneously used. Table 3 reports the results obtained by fitting the same data separately for supramaximal and submaximal stimula-

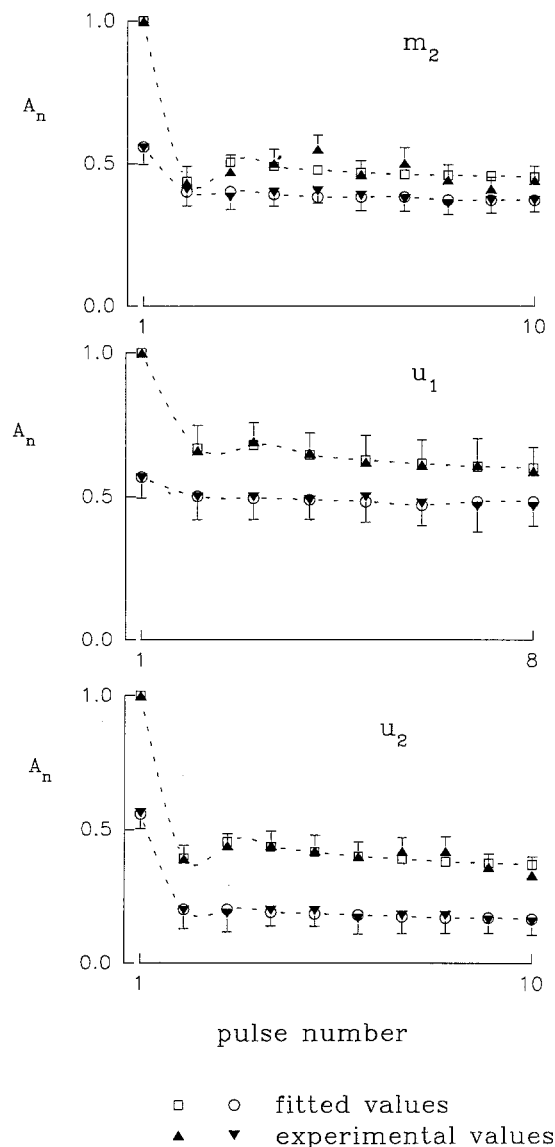


Fig. 6 Plot of experimental (▲, ▼) and simulated (□, ○; see Appendix) fatigue process for m_2 , u_1 and u_2 waves. Theoretical fitting of datapoints was provided by Eqs. A1–A3. Note close correlation between experimental data and computer simulation of fatigue process. *Abscissa*, number of pulses in the 1 Hz train; *ordinate*, amplitude of each response (A_n) normalized to the first one elicited by supramaximal stimulation. In each panel the *top curve* represents responses evoked by supramaximal stimuli while the *bottom curve* shows responses induced by weak pulses ($n=4$). The parameters derived from the best fit were: for the m_2 , $\tau_{NT} = 4.0$ s, $\alpha = 0.94$, $\tau_{inh} = 0.77$ s; for the u_1 , $\tau_{NT} = 3.1$ s, $\alpha = 0.78$, $\tau_{inh} = 0.52$ s; for the u_2 , $\tau_{NT} = 10.5$ s, $\alpha = 0.88$, $\tau_{inh} = 2.1$ s

tions, respectively. A good agreement was found for all parameters except α for the u_1 wave and τ_{NT} for the u_2 wave.

Within the constraints imposed by the choice of the present model, the data of Table 3 allow some quantification of the various processes involved in synaptic fatigue. For example it may be suggested that:

1. Refilling IAS from LTS is virtually completed in about 9–12 s for the m_2 and u_1 waves and about 25–30 s

Table 3 Parameters obtained from the best fit of the experimental data. Mean \pm SEM of the parameters obtained from the best fit from three preparations for each of the waves. The residuals are expressed as: $R = \sqrt{\sum_{k=1, N} [A_{\text{exper}}(k) - A_{\text{theor}}(k)]^2 / N}$ where $A_{\text{exper}}(k)$ and $A_{\text{theor}}(k)$ are experimental and calculated normalized values, respectively (see Fig. 6 legend) with N = number of points. τ_{NT} time constant for neurotransmitter transfer from the LTS to the IAS, α ($0 \leq \alpha \leq 1$) is proportional to the inhibition elicited by each stimulation, τ_{inh} time constant for the decay of inhibition, *Simultaneous* values from simultaneous fit for supramaximal and submaximal stimulations, *Supramaximal*, *Submaximal* values from separate fit for supramaximal and submaximal stimulations, respectively

	τ_{NT} (s)	α	τ_{inh} (s)	R
Simultaneous				
m_2	3.6 ± 1.7	0.70 ± 0.20	1.1 ± 0.6	0.051
u_1	2.9 ± 0.8	0.74 ± 0.13	0.8 ± 0.4	0.035
u_2	8.8 ± 2.2	0.89 ± 0.05	2.0 ± 0.2	0.032
Supramaximal				
m_2	3.7 ± 1.1	0.78 ± 0.17	0.90 ± 0.35	0.034
u_1	4.0 ± 0.5	0.94 ± 0.05	0.79 ± 0.20	0.029
u_2	8.4 ± 2.1	0.90 ± 0.06	3.34 ± 0.90	0.027
Submaximal				
m_2	3.4 ± 1.0	0.67 ± 0.10	0.72 ± 0.28	0.039
u_1	2.6 ± 0.8	0.18 ± 0.04	0.76 ± 0.27	0.033
u_2	4.2 ± 0.8	0.81 ± 0.10	2.3 ± 0.5	0.030

for the u_2 wave, which are intervals three- to fourfold longer than the respective τ_{NT} values.

2. The values of α derived from the best fit are near unity, showing that inhibition may provide an important contribution to fatigue of synaptic transmission.

3. The mean value of τ_{inh} is about 1–2 s for all waves, indicating the involvement of a process faster than neurotransmitter store depletion as the mechanism responsible for the observed depression of early responses.

Discussion

The principal finding of the present study was that fatigue of the excitatory monosynaptic transmission from optic nerve fibres to tectal neurones displayed a complex time course, since a strong reduction in the amplitude of the early responses in a train was followed by a temporary recovery and then a final decline to a steady level. This pattern was not an invariable phenomenon, since experimental manipulations such as lowering the stimulus intensity, reducing $[Ca^{2+}]_o$ or adding the GABA_A receptor antagonist picrotoxin transformed such a complex phenomenon into a smooth decay of synaptic transmission to a steady plateau.

While the isolated frog OT offered particularly advantageous conditions in terms of histological organization and experimental reliability, it should be noted that electrophysiological responses were recorded with extracellular electrodes located in a multisynaptic network. Thus, the present data seem more relevant to understanding the function of the synaptic circuits rather than the molecular processes underlying them. At low

frequencies of optic nerve stimulation there was no decrement in excitatory transmission, but at the 1 Hz rate there was a sharp, early decline (seen as a dip in Figs. 1 and 2), particularly evident when strong presynaptic stimuli were used. These observations suggest that the early dip in synaptic transmission was not caused by lack of synchrony in the activation of presynaptic fibres or temporal failure of the afferent volley (which remained unchanged). The frequency and intensity dependence of the dip phenomenon suggested the possible involvement of an inhibitory circuit. This view was confirmed by the smoother development of fatigue when extracellular Ca^{2+} was lowered and Mg^{2+} was raised (a smaller concentration of Ca^{2+} could not be used without strong block of synaptic transmission). A clue to the possible identity of the inhibitory system was provided by the block of the dip in transmission by picrotoxin, an antagonist of GABA_A receptor mediated responses (Sivilotti and Nistri 1991). Since in an anatomical study of the frog OT (Hughes 1990) less than 20% of the tectal nerve terminals are reported to belong to retinal afferents, it is likely that part of the remaining nerve endings make up an intrinsic network. Several kinds of GABAergic terminal and dendrite identified in an immunohistochemical study (Antal 1991) provide histological evidence for the inhibitory component in a local interneuronal circuitry.

Synaptic fatigue may not be the only short-term change in transmission following repetitive stimulation of retinal afferents. In fact, it is generally accepted that chemical synapses exhibit paired-pulse facilitation when two closely spaced stimuli are applied to presynaptic fibres (Katz and Miledi 1968). In the frog OT a prepulse facilitated the response to a test pulse when the interval was 20–200 ms (this observation applied both to weak and strong pulses). Nevertheless, when the interval extended beyond 500 ms, facilitation was replaced by depression for responses induced by strong pulses, or by little change in amplitude following weak stimuli. These results confirm the presence of paired-pulse facilitation in this preparation and indicate that such a phenomenon did not interfere with synaptic fatigue which was present over a longer time span.

A model was constructed to fit the time course of synaptic fatigue in the frog OT in order to describe this process rather than providing a mechanistic interpretation of it. The present model combines a term accounting for synaptic fatigue as slow refilling of a presynaptic store of excitatory neurotransmitter with a term for an inhibitory process (supposed to be similar to lateral inhibition observed in the *Limulus* eye; Hartline and Ratliff 1972). Presumably, the lag between emptying an immediately available store and its refilling from a long-term store underlies the monotonic reduction in the amplitude of excitatory responses to a steady level, which is determined by the rate of transmitter transfer between the two stores. Using these assumptions, experimentally derived parameters were found to produce a good fit of the observed pattern of fatigue. Simpler models based

only on gradual depletion of presynaptic stores of neurotransmitter were found insufficient to describe experimental data. Notwithstanding the closeness between observed and fitted results, other more complicated models might have been used: for instance, a model which introduced a threshold value at which the inhibitory process became operative and/or which contained a factor related to intrinsic fatigue of the inhibitory system. Computations based on these additional (albeit realistic) assumptions would have required the introduction of other degrees of freedom, leaving in turn the system underdetermined. The simplicity of the present model in simulating rather accurately the development of synaptic fatigue is an obvious advantage, although it cannot entirely explain the observed data. For example, the existence of a threshold for the activation of inhibition, which was left out from the present model, might account for the discrepancy between α values for supramaximal and submaximal stimulations eliciting the u_1 wave. The difference between τ_{NT} after supramaximal or submaximal stimulation might also indicate an additional mechanism causing more severe fatigue elicited by the stronger stimuli. Furthermore, while the model suggests a role for an inhibitory synaptic circuit in shaping fatigue of excitatory transmission, it does not allow a distinction to be made between various types of inhibition (for instance feed-forward or feed-back, or even pre-synaptic).

Acknowledgements We thank Dr. A. Treves for his helpful comments on modelling and Mr. M. Viola for electronic and software support. This work was in part supported by grants from INFM, MURST and EEC "Science" Plan.

Appendix

Assuming that synaptic fatigue was produced by a combination of the slow refilling of presynaptic stores simultaneously with the onset of local inhibition, the following iterative equation was used to describe the time course of synaptic fatigue:

$$A_n = kc_n - \alpha I_n \quad (\text{A1})$$

where A_n , the amplitude of the n^{th} waveform normalized to the first supramaximal response, is the difference between two terms, the first one accounting for the repletion of IAS from LTS, and the second one representing the inhibitory process. k (proportional to the amplitude of the first response) is the constant fraction of neurotransmitter concentration released by each pulse, and α ($0 \leq \alpha \leq 1$) is a constant which accounts for the total amount of inhibition. c_n is the (variable) neurotransmitter concentration in the IAS just before the n^{th} stimulation and is given by:

$$c_n = c_{n-1} + (c_0 - c_{n-1})(1 - e^{-(\delta t/\tau_{NT})}) \quad (\text{A2})$$

where c_0 is the asymptotic value for the neurotransmitter concentration in the IAS, τ_{NT} is the time constant for

refilling IAS from LTS, and δt is the interpulse delay. I_n is the fraction of inhibition acting on the n^{th} response and is given by the following expression:

$$I_n = I_{n-1}e^{-(\delta t/\tau_{\text{inh}})} + A_{n-1}(1 - I_{n-1})e^{-(\delta t/\tau_{\text{inh}})} \quad (\text{A3})$$

where τ_{inh} is the time constant for intrinsic decay (supposed to be exponential) of the inhibitory neurotransmission. In Eq. A3 the first term corresponds to the cumulative inhibition present immediately before the n^{th} pulse, whereas the second term is the inhibition brought about by the n^{th} stimulus itself. Each time the IAS neurotransmitter concentration is suddenly depleted by a pulse, its refilling from the LTS follows a first-order kinetic given by the value of c_n from eq. A2.

The initial condition for the iterative equation is given by: $I_0=0$, $A_0=0$, corresponding to absence of inhibition at the first response.

References

- Antal M (1991) Distribution of GABA immunoreactivity in the optic tectum of the frog: a light and electron microscopy study. *Neuroscience* 42:879–891
- Chung SH, Bliss TVP, Keating MJ (1974) The synaptic organization of optic afferents in the amphibian tectum. *Proc R Soc Lond [Biol]* 187:421–447
- Colquhoun D (1971) *Lectures on biostatistics*. Clarendon, Oxford, pp 160–170
- Hartline HK, Ratliff F (1972) Inhibitory interaction in the retina of *Limulus*. In: Fuortes MGF (ed) *Handbook of sensory physiology*. Springer, Berlin Heidelberg New York, pp 381–447
- Hughes TE (1990) A light- and electron-microscopic investigation of the optic tectum of the frog, *Rana pipiens*. I. The retinal axons. *Vis Neurosci* 4:519–531
- Katz B, Miledi R (1968) The role of calcium in neuromuscular facilitation. *J Physiol (Lond)* 195:481–492
- Lázár G (1984) Structure and connections of the frog optic tectum. In: Vanegas H (ed) *Comparative neurology of the optic tectum*. Plenum, New York, pp 185–210
- Llinás R, Steinberg IZ, Walton K (1981) Relationship between presynaptic calcium current and postsynaptic potential in squid giant synapse. *Biophys J* 33:323–352
- Maddess T, McCourt ME, Blakeslee B, Cunningham RB (1988) Factors governing the adaptation of cells in area 17 of the cat visual cortex. *Biol Cybern* 59:229–236
- Magleby KL (1987) Short term changes in synaptic activity. In: Edelman GM, Gall WE, Cowan WM (eds) *Synaptic function*. Wiley, New York, pp 21–56
- Maturana HR, Lettvin JY, McCulloch WS, Pitts WH (1960) Anatomy and physiology of the vision in the frog. *J Gen Physiol [Suppl]* 43:129–170
- Nistri A, Sivilotti L, Welsh DM (1990) An electrophysiological study of the action of *N*-methyl-D-aspartate on excitatory synaptic transmission in the optic tectum of the frog in vitro. *Neuropharmacology* 29:681–687
- Sivilotti L, Nistri A (1991) GABA receptor mechanisms in the central nervous system. *Progr Neurobiol* 36:35–92
- Vidyasagar TR (1990) Pattern of adaptation in cat visual cortex is a co-operative phenomenon. *Neuroscience* 36:175–179